RAPID COMMUNICATIONS

PHYSICAL REVIEW E VOLUME 48, NUMBER 3 SEPTEMBER 1993

Measurement of the persistence length of polymerized actin using fluorescence microscopy

A. Ott,*† M. Magnasco,‡ A. Simon,* and A. Libchaber*
NEC Research Institute, 4 Independence Way, Princeton, New Jersey 08540
(Received 2 June 1993)

Single actin filaments were confined between bovine-serum-albumine-coated glass plates, with a separation of about 1 μm, and their flickering Brownian movement was observed by fluorescence microscopy. The rigidity of the filaments was measured by extracting the correlation function given by the mean dot product between unit tangent vectors of an isolated filament. The result is consistent with current rigidity values found in the literature.

PACS number(s): 87.10.+e, 83.10.Nn

Actin plays an important and multifunctional role in biological organisms. Examples of its functions are force generation in muscles [1], cell mobility driven by gel-sol transitions of an actin network [2], and the formation of filopodia due to actin polymerization involved in neuronal growth [3]. Filamentous actin (f-actin) is a two-stranded 8-nm-diam helix, with a repeat distance of about 40 nm. It is made of polymerized protein subunits of actin monomers. Actin filaments can become very long, up to the order of 100 μm; they are semiflexible polymers on the micrometer scale. The persistence length of actin is very long compared to synthetic polymers and hence actin is one of the very few semiflexible polymers that can be visualized in isolation by video microscopy. We report such observations of fluorescently labeled actin and show how the persistence length can be extracted. We compare our result to literature values obtained by other techniques. We also compare our work to other measurements using fluorescence microscopy: our value of the persistence length is in agreement with the result of Gittes *et al.* [4]. However, our findings do not agree with those of Kaes *et al.* [5]. Not only does our value for the persistence length differ by a factor of 2 [6], but also and more importantly, we do not observe a wave-vector-dependent bending stiffness.

In order to keep the actin filaments within the focal plane of the microscope, they had to be confined to two dimensions. We therefore constructed a cell with a thickness comparable to the focal depth of our microscope, which is about 1 μm. Since the cover slip of a typical cell is thin and flexible, a controlled spacing between slip and slide is difficult to obtain. In order to stabilize the cover slip, we curved it slightly and used a few glass beads of 1.6 μm diameter as spacers (Fig. 1). The thickness of the so-constructed cell was measured by counting the Newton fringes appearing in daylight. It was found to be a simple way to obtain a spacing between 1 and 1.5 μm. In order to avoid sticking of the actin filament to the glass surfaces, these were coated with bovine serum albumin (BSA). The plates were dipped into a 1-mg/ml BSA solution and slowly extracted using a motor (1 mm/min). They were dried before assembly of the cell. Once assembled the cell was filled by capillarity and sealed using Elmer's superfast epoxy glue.

Actin was purified from White Leghorn Chicken breast following a published procedure [7]. The experiments were performed in actin suspension buffer containing 25.0 m*M* Imidazole and 25.0 m*M* KCl adjusted to *p*H 7.65 by adding HCl. For fluorescent labeling, actin was suspended overnight in the presence of rhodamine labeled phalloidin [8] and then centrifuged to get rid of unbound rhodamine dye to avoid background fluorescence [9]. We obtain a distribution of actin polymer length up to 30 μm. It would be desirable to have longer filaments but it is our experience that they are not very stable and break easily as the sample is filled.

Observations were made on a Zeiss Axioscop equipped with a 50-W mercury lamp, 63X Plan Apochromat objective, and a standard filter set [10]. To avoid photobleaching during observation, 1 mg/ml glucose, 33 units/ml glucose oxidase [11], 50 units/ml catalase, and 0.3 mg/ml dithiotheitol (DTT) were added to the actin solution just before filling the cell. Also to prolong observation time, the excitation light intensity was reduced in the beginning of the observation by inserting pinholes. This made it possible to observe the Brownian movement of the filaments during 20 min. Otherwise fluorescence decayed on the order of seconds and was followed generally by break-

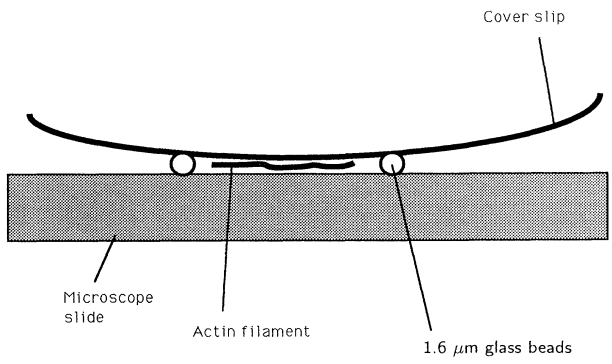

FIG. 1. Schematic of the cell used to confine the actin filaments; the scales are not respected. In the region of observation the thickness is between 1 and 1.5 μms.

age of the filaments. Experiments were performed at room temperature and at a concentration of 10 nM of rhodamine phalloidin labeled actin. Images were recorded through a 4× TV tube via an image intensifier followed by a Newvicon camera [12] connected to an NEC S-VHS recorder, corresponding to an overall screen size of 82 μm in horizontal dimension and a resolution of 0.14 μm/pixel. Data were digitized by first transferring them to a Sony videodisc, and then to a Silicon Graphics Crimson VGX workstation via a Silicon Graphics VideoLab Interface. The videodisc allows fully automatic frame grabbing with optimal image stability.

Figure 2 shows a recorded actin filament in different conformations. Twenty thousand consecutive frames (11 min) of data were analyzed, frame by frame, including all the filaments in each frame. We first computed the average and standard deviation of pixel values. Since the brightly fluorescent pixels which constitute the filament are a minority of the entire field of view, their intensity values do not produce a distinct peak in a histogram. We therefore separated "foreground" from "background" by choosing a threshold level equal to the mean pixel value plus three standard deviations, producing a binary image. The "worms" obtained in this fashion have a thickness of about eight pixels corresponding to roughly 1 μm in real space. We skeletonized these thick objects by a recursive process. A circle of radius three pixels was drawn around each pixel in the "worm"; the center of mass of the intersection of this disk with the worm defines a "new" pixel position (Fig. 3). This is a contractive transformation which eventually reduces the thickness to a one-pixel skeleton (Fig. 4). An arclength reparametrization of this skeleton was constructed by drawing a circle of radius r_p, beginning at one tip, and finding the intersection with the filament. This intersection is used as the center for the next circle unit until the filament is covered (Fig. 5). Using this choice of successive vectors of equal length, we compute their correlation by direct convolution.

Theory predicts for an ideal polymer [13] that the

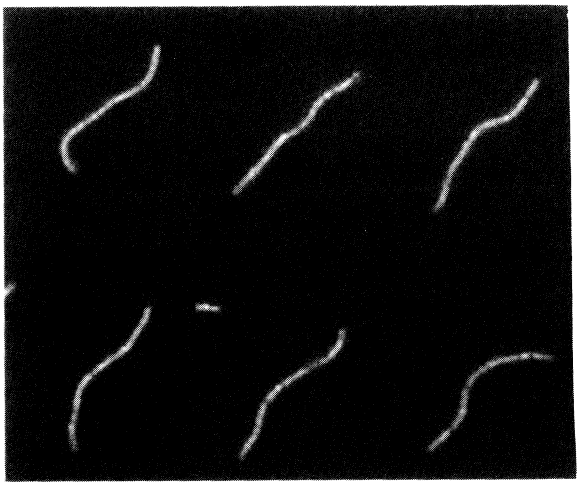

FIG. 2. An actin filament as observed by video fluorescence microscopy at time intervals of 10 s. (Successive images from left to right then top to bottom.)

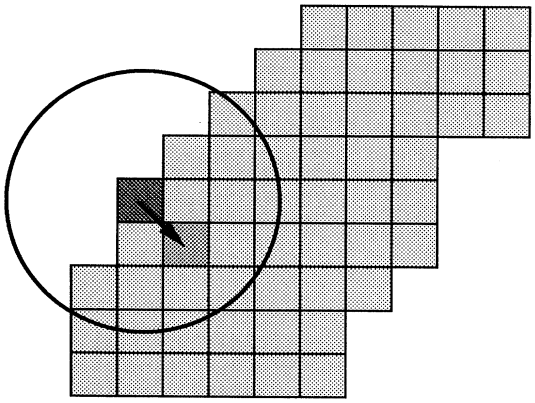

FIG. 3. Contraction of the filament: A circle of radius three pixels is drawn around each pixel of the "worm"; the center of mass of the intersection of this disk with the worm defines a "new" pixel position (arrow). Successive application of this transformation leads to a one-pixel-thick skeleton.

mean dot product between unit tangent vectors [the "cosine correlation function" (CCF)] in the case of two-dimensional confinement is given by

$$\langle \mathbf{t}(s)\cdot\mathbf{t}(s+x)\rangle = \exp(-x/2L_p)\ , \qquad (1)$$

where x is the distance from the initial position s along the filament and L_p is the persistence length. Figure 6 shows the CCF for four different values of the reparametrization parameter r_p (three, five, seven, and nine pixels) on a semilog plot. Notice that varying r_p moves the curves up and down, but that in the central portion of the figure the slope is unaffected. One concludes that absolute amplitudes are not to be trusted since they are reparametrization dependent, but nevertheless the slopes can be used to determine L_P. Note that each curve is a single exponential and no deviation on a length scale between 5 and 15 μm could be detected within the experimental uncertainty. Deviations outside this region are due to finite pixel size effects at short distances (<5 μm) and statistical bias due to a lack of long filaments at long distances (>15 μm). The measured slope of 33.5 μm^{-1} leads to a persistence length of

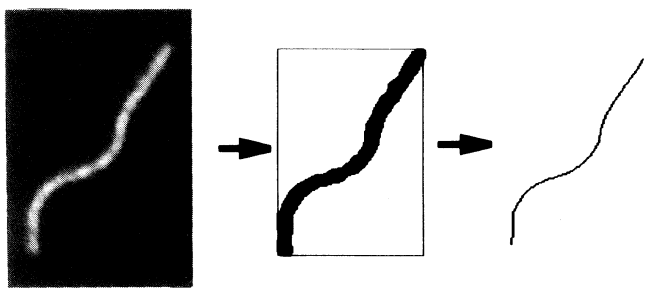

FIG. 4. From left to right: Actin filament as seen on the screen; after thresholding as a binary image; after reduction to a one-pixel-wide skeleton following the procedure illustrated in Fig. 3.

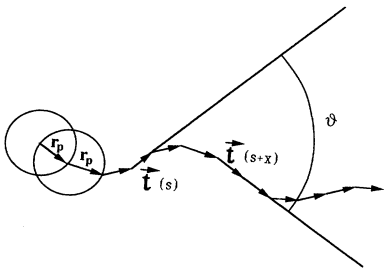

FIG. 5. An arclength reparametrization of a skeleton is constructed by drawing a circle of radius r_p, beginning at one tip, and finding the intersection with the filament. This intersection is used as the center for the next circle until the filament is covered.

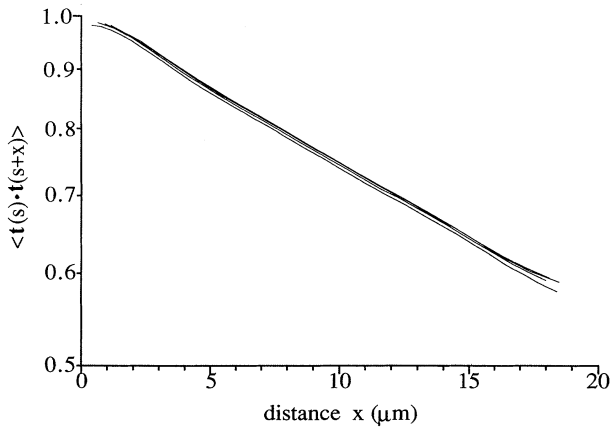

FIG. 6. Cosine correlation function (CCF) on a semilog plot for different values of the reparametrization parameter r_p shown in Fig. 5. The curves correspond to values of r_p of three, five, seven, and nine pixels (from top to bottom).

$L_p = 16.7 \pm 0.2$ μm. The error is given by assuming that the true curve lies anywhere between the CCF's obtained from the extreme values of the reparametrization parameter r_p. We were unable to investigate the effect of the random potential causing friction between the filament and the BSA-coated glass surfaces. However, no effect of pointwise sticking of the filament could be detected for a short time series in the analysis of the data.

Previous work using static measurements of the end-to-end distance [14,15], or micromechanical measurements of the bending stiffness [16], led to a value between 6 and 25 μm, which given the precision of such measurements is in reasonable agreement with our result. Recently Gittes *et al.* [4] found a value of $17.5 \pm 1.1 +$ μm also using fluorescence microscopy, but performing a mode analysis. Since the fluctuation spectrum is a Fourier transform of the CCF, we expect the amplitudes of the modes to have substantial dependence upon r_p, and hence intrinsic error. The inaccuracy of the mode amplitude measurement does not permit one to conclude about eventual deviations from the ideal case. Our value also agrees with an unpublished estimation by Maggs and Leibler [17] derived from the end-to-end distance and maximal width fluctuations.

Kaes *et al.* [5], also using fluorescence microscopy, performed a mode analysis. However, for microscopic observation they used a cell of 10–15-μm thickness. This means that the actin filaments were not confined to the focal plane of the microscope. Only those videoframes where the whole given filament was in focus were used for further analysis. Their results differ from our observations. Not only does our value for the persistence length differ by a factor of 2 [6] but also and more importantly, a wave-vector-dependent bending stiffness would lead to a nonexponential CCF, contrary to our observation. Let us note that Kaes *et al.* observe sharp bends along the filament and we do not.

Protein polymers have complex monomers. It is thus important to verify that they behave like simple "Flory-type" polymers. This is the case for our observations of filamentous actin: they show that it can be described as a semiflexible polymer using the persistence length as a reasonable measure. We found a persistence length of $L_p = 16.7 \pm 0.2$ μm. This measurement should be seen as an important step leading to a unified description of the rheology of actin solutions. Such a framework has been proposed by Cates [18] in a model for "living" polymers, i.e., polymers that may break and recombine.

We would like to thank D. A. Winkelmann and his group, without whom the actin purification would have become a difficult task, and T. Maggs and S. Leibler for helpful discussions. D. Smith performed some initial experiments. A. Ott acknowledges CNRS funding.

*Also at Department of Physics, Princeton University, Princeton, NJ 08544.

†On leave from Ecole Normale Supérieure, Paris, France.

‡Also at Physics Department, Rockefeller University, New York, NY 10021.

[1] E. Eisenberg and T. L. Hill, Science **227**, 999 (1985).

[2] P. Madsudaira and P. Janmey, The Cell **54**, 139 (1988).

[3] S. J. Smith, Science **242**, 708 (1988).

[4] F. Gittes, B. Mickney, J. Nettleton, and J. Howard, J. Cell Bio. **120**, 923 (1993).

[5] J. Kaes, H. Strey, M. Baermann, and E. Sackmann, Europhys. Lett. **21**, 865 (1993).

[6] The published value of 0.5 μm should be corrected to 8 μm. J. Kaes (private communication).

[7] J. Pardee and J. A. Spudich, Methods Enzymol. **85B**, 164 (1982).

[8] Rhodamine phalloidin R-415, Molecular Probes, Eugene, OR.

[9] D. A. Winkelman, F. Kinose, and A. L. Chung, J. Muscle Res. Cell Motility (to be published).

[10] Omega Optical rhodamine phalloidin filter, Catalog Nos. 540DF23, 605DF55, and 600ELFP.

[11] Using the unit definition from Sigma Chemical.
[12] Hamamatsu HAC240-07 Newvicon Camera combined with a Hamamatsu C2400-68 Intensifier Head.
[13] M. Doi and S. F. Edwards, *The Theory of Polymer Dynamics* (Clarendon, Oxford, 1986), p. 317.
[14] T. Yanagida, M. Nakase, K. Nishiyama, and F. Oosawa, Nature **307**, 58 (1984).
[15] T. Takebayashi, Y. Morita, and F. Oosawa, Biochim. Biophys. Acta. **492**, 357 (1977).
[16] A. Ishijima, T. Doi, K. Sakurada, and T. Yanagida, Nature **352**, 301 (1991).
[17] T. Maggs and S. Leibler (private communication).
[18] M. E. Cates, Macromolecules **20**, 2289 (1987); J. Phys. (Paris) **49**, 1593 (1988).

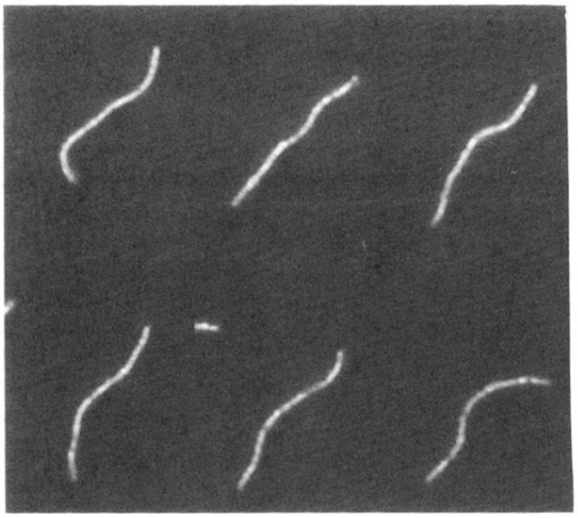

FIG. 2. An actin filament as observed by video fluorescence microscopy at time intervals of 10 s. (Successive images from left to right then top to bottom.)

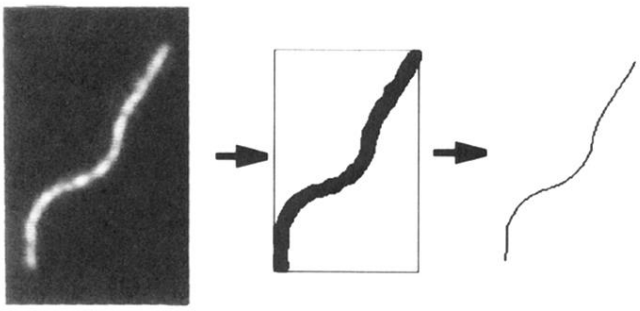

FIG. 4. From left to right: Actin filament as seen on the screen; after thresholding as a binary image; after reduction to a one-pixel-wide skeleton following the procedure illustrated in Fig. 3.